

**“Electric field induced birefringence in non-aqueous dispersions of
mineral nanorods”**

Alexis de la Cotte,¹ Pascal Merzeau,¹ Jong Wook Kim,² Khalid
Lahlil,² Jean-Pierre Boilot,² Thierry Gacoin,² and Eric Grelet^{1,*}

¹*Centre de Recherche Paul-Pascal, CNRS - Université de Bordeaux,
115 Avenue Schweitzer, 33600 Pessac, France*

²*Laboratoire de Physique de la Matière Condensée,
CNRS - Ecole Polytechnique, 91128 Palaiseau, France*

(Dated: July 6, 2015)

* grelet@crpp-bordeaux.cnrs.fr

I. MEASUREMENTS OF THE KERR COEFFICIENTS AT DIFFERENT VOLUME FRACTIONS AND ELECTRIC FIELD FREQUENCIES

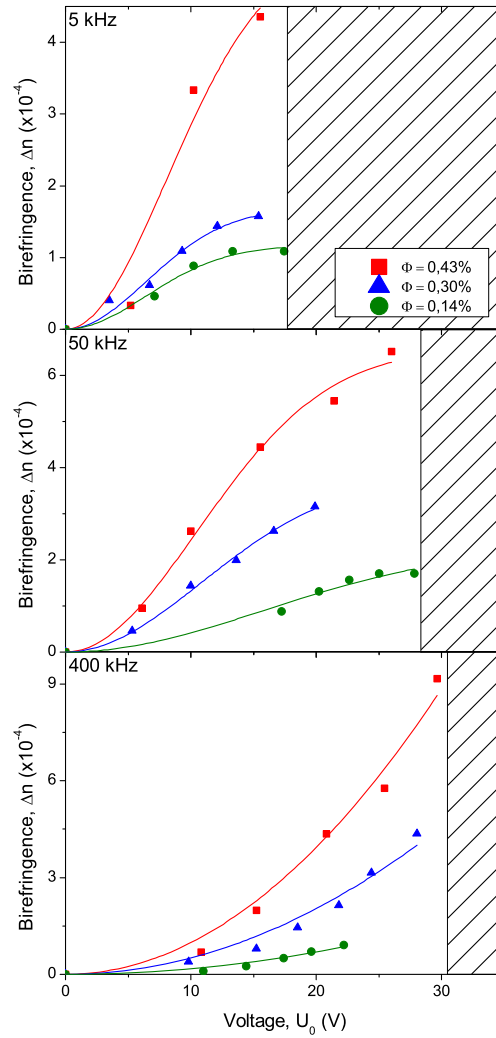


FIG. S1. Kerr induced birefringence in IPS cells for three volume fractions of 0.43%, 0.30% and 0.14% corresponding to square, triangle and circle symbols, respectively. An a.c. sinusoidal electric field was applied at three different voltage frequencies (5, 50 and 400 kHz). The dashed areas correspond to the range of electric fields above which electric damage of the sample occurs in the IPS cells.

Figure S1 shows the evolution of the Kerr induced birefringence for different conditions of volume fraction (0.43%, 0.30% and 0.14%) and voltage frequencies (5, 50 and 400 kHz). The lines corresponds to numerical fits using Eqs. 4 and 5 from which the Kerr coefficients displayed in Figure 6 of the paper are extracted.

II. ATTENUATION OF THE ELECTRIC FIELD IN THE CAPILLARY SETUP OBTAINED BY NUMERICAL SIMULATIONS

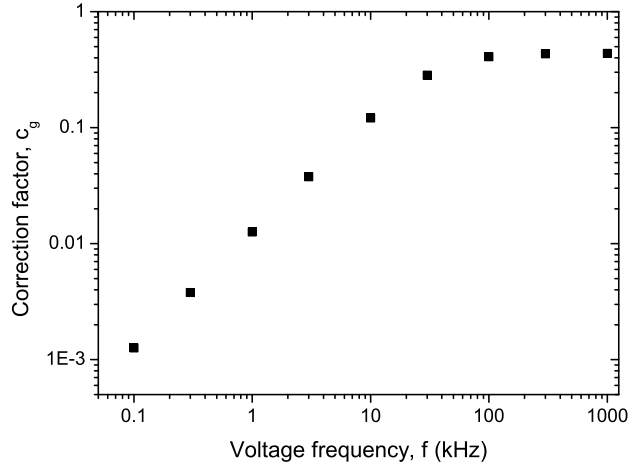


FIG. S2. Evolution of the correction factor c_g with the voltage frequency (f) obtained from finite element simulations in the geometry of externally applied filed through a quartz capillary. The inter-electrode distance (d) is fixed at $500 \mu\text{m}$ and the electrolyte conductivity $K_e = 4 \times 10^{-4} \text{ S/m}$.

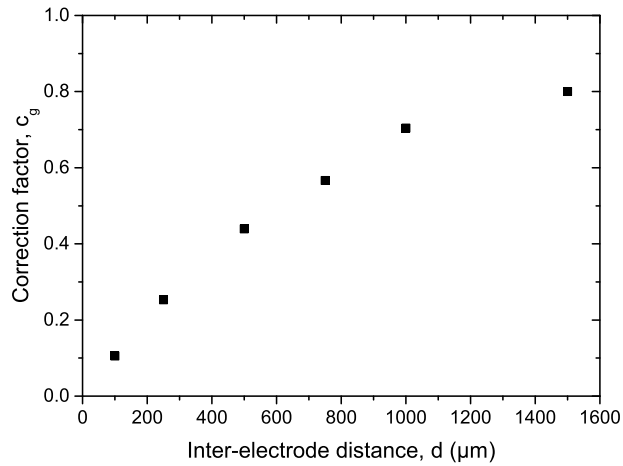


FIG. S3. Correction factor c_g as a function of the inter-electrode distance (d) obtained from numerical simulations in the geometry of externally applied filed through a quartz capillary. The voltage frequency (f) is fixed at 100 kHz and the electrolyte conductivity $K_e = 4 \times 10^{-4} \text{ S/m}$.

The correction factor c_g (Eq. 1) in the capillary geometry is dependent on both the inter-electrode distance (d) and voltage frequency (f) due to the presence of an insulating quartz wall between the electrode and the sample. To quantify this attenuation, the electric

field has been simulated by finite element analysis (QuickField software, Student Edition) for different parameters d and f and the results are presented in Figs. S2 and S3. Due to a limited number of meshes in this free edition, the numerical simulations of the thin quartz wall ($e_{\text{quartz}} = 10 \mu\text{m}$) were carried out, replacing it by an equivalent material of larger thickness and effective dielectric constant and keeping unchanged their ratio ($e_{\text{eff}}/\varepsilon_{\text{eff}} = e_{\text{quartz}}/\varepsilon_{\text{quartz}} = \text{constant}$). At low frequencies, capacitive impedances are prevailing and the correction factor c_g increases with f while at high frequencies, the predominance of resistive impedances makes its behavior asymptotic (Fig. S2). In the same way, at short distances c_g increases with d until an asymptotic behavior is reached for high enough inter-electrode distances (Fig. S3) for which c_g tends to 1. Such a behavior obtained by simulations is in qualitative agreement with the experimental data shown in Fig. S4.

III. KERR COEFFICIENT MEASUREMENTS IN THE GEOMETRY OF EXTERNALLY APPLIED ELECTRIC FIELD (QUARTZ CAPILLARY)

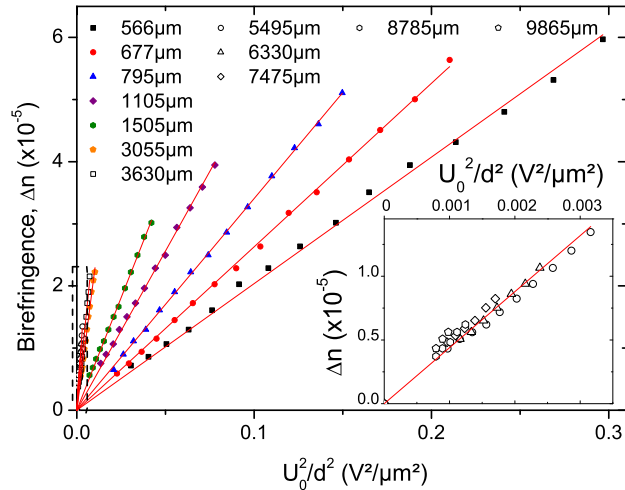


FIG. S4. Kerr induced birefringence as a function of the applied voltage ($f = 100 \text{ kHz}$) for varying inter-electrode distance d in the geometry of quartz capillary and for $\Phi=0.66\%$. The inset corresponds to a zoom of the area (dashed box) where the slopes overlap, corresponding to an homogeneous electric field with no attenuation ($c_g = 1$). The symbols represent the experimental data and the solid lines the numerical linear fits.

In order to determine the Kerr coefficient in the capillary setup, several sets of measure-

ments have been performed at different inter-electrode distances. Thanks to the diameter of the cylindrical capillary (1 mm) the optical retardation increases accordingly (Eq. 2) allowing for a field induced birefringence measurement up to large inter-electrode distances (of about 10 mm). Note that all birefringence values have been corrected from an offset coming from some residual birefringence attributed to some mechanical stress on the capillary glass wall. Figure S4 shows the evolution of the measured birefringence with the square of the applied voltage for the different distances and the corresponding linear fits. This dependence demonstrates that the response of the system is in the weak field regime ($E \ll E_{sat}$) according to Eq. 5.

The presence of a progressive increase followed by an overlap of the slopes (for $d \geq 5$ mm) is in qualitative agreement with the numerical simulations in Figure S3 showing the attenuation of the electric field vanishes at high enough inter-electrode distance d . Therefore, for the largest distances where the field is homogeneous ($c_g = 1$) and for which $E = U/d$ applies (inset of Figure S4), the value of the Kerr coefficient can be extracted for our system in this specific cell and is reported in Fig. 7.

IV. ZETA-POTENTIAL MEASUREMENTS

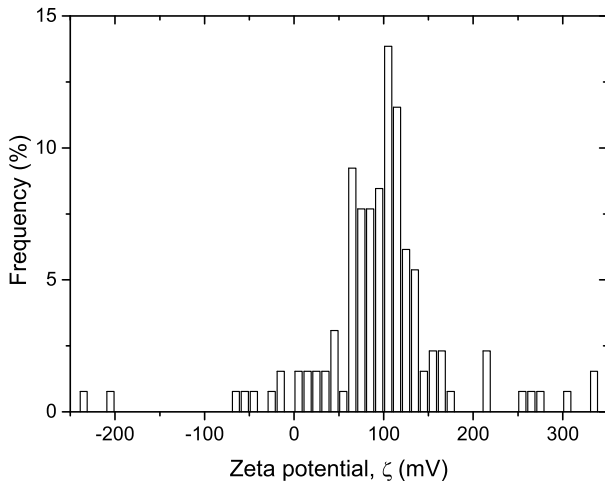


FIG. S5. Zeta-potential (ζ) measurements on a population of 130 particles performed under a steady-state electric field (14.6 V/cm) in the dilute state.

Zeta-potential (ζ) measurements were made using a particle electrophoresis instrument (Zeta Compact, CAD Instruments) and are presented in Figure S5. The velocity and di-

rection of the rods are measured by recording their movement under a steady-state electric field (14.6 V/cm) in a dilute suspension thus providing their mobility. The zeta-potential is then deduced using Smoluckowski equation beyond its range of strict validity corresponding to $\kappa R \gg 1$. The ζ value is the mean for all the particles in the field of view, and has been averaged over several measurements to provide $\zeta = +97$ mV.

V. SHORTCIRCUIT VOLTAGE IN THE IPS CELLS

The voltage at which shortcircuits occur in the IPS cell has been measured for the three studied frequencies (5, 50 and 400 kHz) in ethylene glycol electrolyte with and without LaPO_4 nanorods. Three sets of measurements were performed: pure ethylene glycol, ethylene glycol whose conductivity has been adjusted by adding CsNO_3 salt to match the conductivity of our LaPO_4 suspensions ($K_e \simeq 5 \times 10^{-4} \text{ S/m}$), and LaPO_4 suspensions. Results are shown in Table S1.

TABLE S1. Voltage at which shortcircuit occur in the IPS cell (U_{sc}) at the three frequencies (5, 50 and 400 kHz), for pure ethylene glycol, for ethylene glycol with added salt of CsNO_3 , and for LaPO_4 suspensions.

Frequency (kHz)	$U_{sc}(V)$		
	Pure ethylene glycol	Ethylene glycol with CsNO_3 salt	LaPO_4 suspensions.
5	58.0	31.5	21.5
50	76.0	40.5	26
400	89.0	51.0	30

These experiments confirm therefore that shortcircuits do not directly depend on the dispersed nanoparticles, but mainly stem from the electrolyte itself (and more specifically from its ionic conductivity).